Fracture Mechanics of Concrete and Concrete Structures - Assessment, Durability, Monitoring and Retrofitting of Concrete Structures- B. H. Oh, et al. (eds)
ⓒ 2010 Korea Concrete Institute, Seoul, ISBN 978-89-5708-181-5

Crack propagation analysis due to rebar corrosion

H. Nakamura, K.K.Tran, K.Kawamura & M. Kunieda
Department of Civil Engineering, Nagoya University, Japan.

ABSTRACT: Cracking behavior due to rebar corrosion for concrete specimen with single rebar was evaluated experimentally and analytically. In the experiment, the propagation of crack was observed by the electric corrosion test. Three-dimensional Rigid- Body-Spring-Method (RBSM) with three phase material corrosion expansion model was applied to simulate internal cracking patterns, surface crack width propagation and internal crack propagation. The effect of corrosion products properties and the penetration of corrosion products into cracks during the corrosion process were investigated and cracking behavior due to rebar corrosion was simulated reasonably. As the results, the mechanism of surface crack width propagation with internal crack propagation was clarified.

1 INTRODUCTION

Cracking of concrete due to rebar corrosion is one of the major deterioration behaviors and it causes the spalling of concrete cover or acceleration of deterioration. It is necessary to predict the internal damage from the observable surface condition during maintenance process. Therefore, it is desirable to establish a prediction method to quantitatively assess the internal crack propagation behavior and rebar corrosion rate from surface cracks. The internal crack patterns due to rebar corrosion considering the difference of cover thickness or diameter of reinforcing bar were clarified (Andrade et al., 1993, Cabrera 1996). However, the relationships between propagation of surface and internal cracks as well as progress of surface crack width have not been clear.

In this study, the crack propagation behavior is investigated both analytically and experimentally. In the experiment, the propagation of crack is observed by the electric corrosion test. Then, surface crack widths are measured and internal crack patterns are observed at several rebar corrosion rates. On the other hand, the crack propagation behavior is simulated using Rigid-Body-Spring-Method with three-dimensional Voronoi particles. In the analysis, the three phase material model which consists of rebar, corrosion products layer and concrete is proposed. For the corrosion products layer, the stiffness of corrosion products is considered by initial strain problem due to corrosion expansion. Moreover, the effect of penetration of corrosion products into cracks during corrosion process is considered. The applicability of the model is verified by comparing with the test results. As the results, the progress of surface crack width, the propagation behavior of internal cracks, and the effect of internal cracks to the surface crack width and so on are clarified.

2 EXPERIMENTAL STUDY

2.1 *Testing method*

Dimensions of the specimen with single rebar are shown in Figure 1. Two types of specimen are carried out. Type C30 has concrete cover thickness of 30mm. Type C10 has 10mm cover thickness. There are six specimens in type C30 and one specimen in type C10.

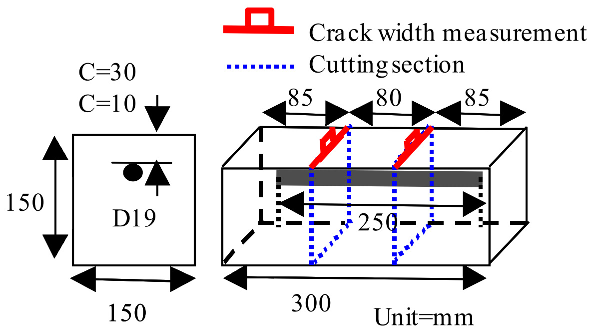

Figure 1. Specimen setup.

In order to accelerate the corrosion process, an external direct electric current density 900μA/cm^2 is applied after 32 days from the casting. Schematic of electric corrosion test is shown in Figure 2.

At the testing time, concrete compressive strength and tensile strength are 18.5 MPa and 1.53 MPa respectively. During the test, surface crack widths are recorded using crack gauges and crack widths are logged in computer files. Testing time is varied for six specimens of type C30 to investigate the effect of corrosion rate to crack patterns and crack width propagation. When the test has been finished, specimens are cut off along the positions shown in Figure 1 to observe internal crack patterns and measure internal crack widths and lengths.

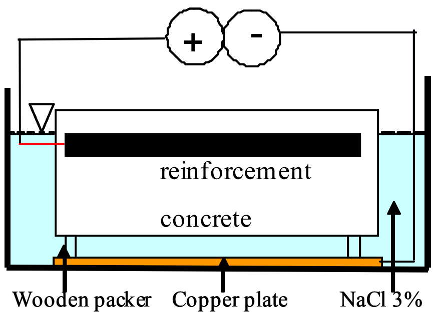

Figure 2. Schematic of corrosion test.

Corrosion rate W_r (mg/cm^2) during the testing is calculated by dividing mass loss W(mg) by wet surface of rebar (cm^2).

$$W_r = \frac{W}{\pi D \cdot L} \tag{1}$$

where D and L are bar diameter (cm) and bar length (cm) respectively.

Mass loss W(g) is calculated by using the following empirical formula based on test results as shown in Figure 3:

$$\begin{aligned} W &= 0.235 I \cdot T && (I.T < 66) \\ W &= 0.617 I \cdot T - 25.305 && (I \cdot T > 66) \end{aligned} \tag{2}$$

where I and T are current intensity (A) and testing time (hour) respectively.

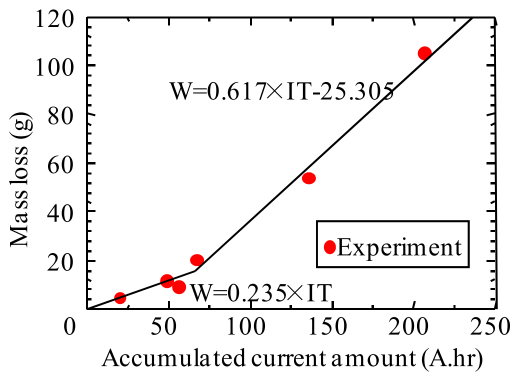

Figure 3. Rebar mass loss computation.

2.2 *Experimental crack patterns*

Figure 4 indicates the defined internal crack types shown in crack patterns.

Internal crack patterns at several corrosion rates of type C30 are shown in Figure 5.

Initiation of visible crack occurs on the surface of concrete cover (vertical crack). When corrosion products increase, the crack propagates inside the concrete cover. After that, lateral cracks appear and their lengths increase. With further amount of corrosion products, inside crack initiates and propagates inside the specimen from the rebar.

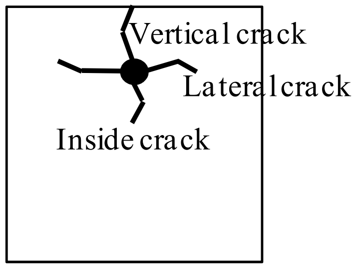

Figure 4. Internal crack types.

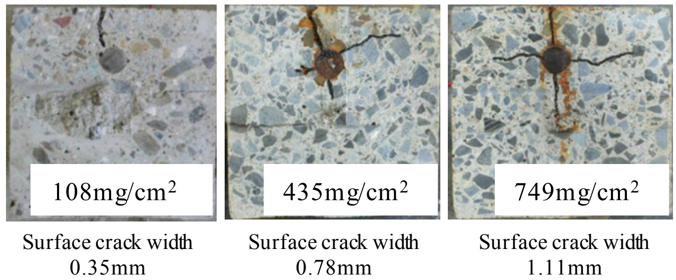

Figure 5. Type C30 crack patterns.

In the case of 10mm cover thickness (type C10), two cracks appear on concrete surface and propagate to the rebar. Then, lateral cracks occur when amount of corrosion products increase as shown in Figure 6.

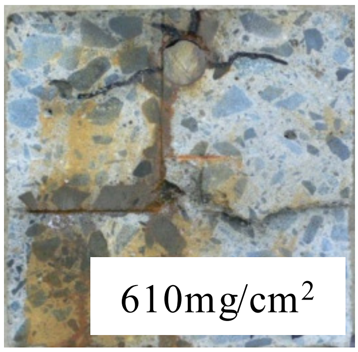

Figure 6. Type C10 crack pattern.

2.3 *Surface crack width propagation*

In the case of 30mm cover thickness (type C30), propagation of surface crack width against corrosion rates at different rebar mass loss levels is shown in Figure 7. It can be seen that opening of surface crack initiates after a significant amount of corrosion products are formed. It can be explained that a critical corrosion amount of corrosion products is required to build up enough expansion stress and to cause cracking in concrete as B.H.Oh discussed about the value (Oh et al. 2009). After the initiation, surface crack width propagates rapidly up to the value of 0.4mm. After that, the speed of propagation reduces with occurrence of lateral cracks and effect of penetration of corrosion products into cracks which is discussed in the later part of the present paper. Moreover, the speed of propagation increases again with the propagation of the inside crack.

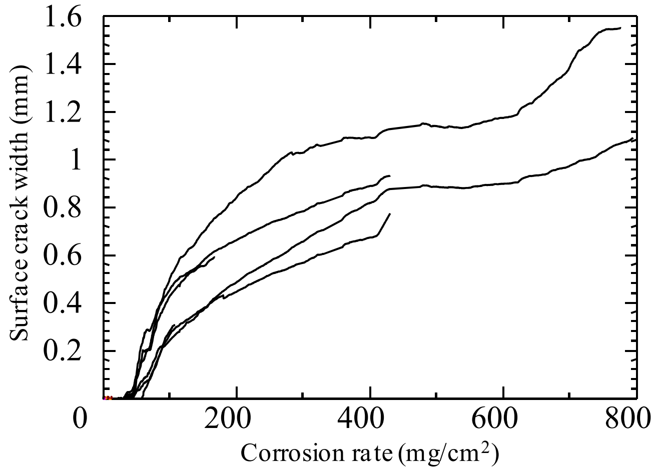

Figure 7. Type C30 surface crack width propagation.

3 ANALYTICAL MODEL

3.1 *Three- dimensional RBSM*

Rigid- Body-Spring-Method (RBSM) is one of the discrete approaches, which are used as structural analysis, since it is easy to deal with crack propagation of concrete directly. The method represents a continuum material as an assemblage of rigid particle elements interconnected by zero springs along their boundaries (Fig. 8). In this study, three-dimensional RBSM is applied. Each element has six degrees of freedom at center points. Boundary between two elements is divided into triangles formed by the center and vertices of the boundary. At each center point of triangle, three springs, one normal and two shear springs are set. The analytical model is divided into elements using Voronoi random polygons. In RBSM model, crack widths can be automatically measured during the analysis. The three-dimensional model is possible to simulate complicated problems.

3.2 *Material model*

Figure 9 shows concrete material models which are used in analysis.

In the compressive model, f'_c is compressive strength of concrete, G_{fc} compressive fracture energy, E_c is Young modulus of concrete.

The tensile behavior of concrete up to the strength is modeled by using linear elastic. While bilinear softening branch of 1/4 model is assumed after cracking as shown, in which f_t is tensile strength, G_{ft} is tensile fracture energy and h is distance between centers of Voronoi elements.

Tangential springs represent the shear transferring mechanism of concrete. The shear strength is assumed to follow the Morh- Coulomb type criterion with the tension and compression caps. The shear fracture criterion is expressed as follows (Saito. 1999):

$$\frac{\tau^2}{\tau_f^2} \geq 1 \tag{3}$$

where

$$\tau_f = \begin{cases} c - \sigma \tan\phi, \, for \sigma \geq 0.5 f'_c \\ c - 0.5 f_c \tan\phi, \, for \sigma < 0.5 f'_c \end{cases} \tag{4}$$

Rebar is modeled as linear elastic.

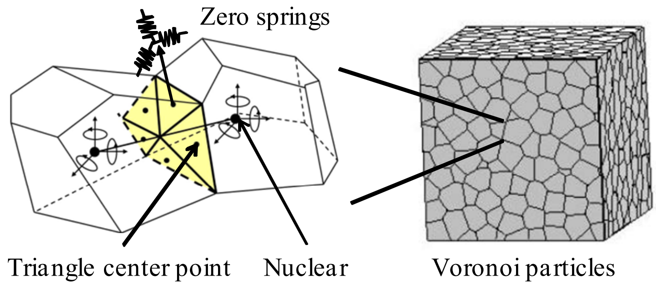

Figure 8. RBSM Voronoi polygons.

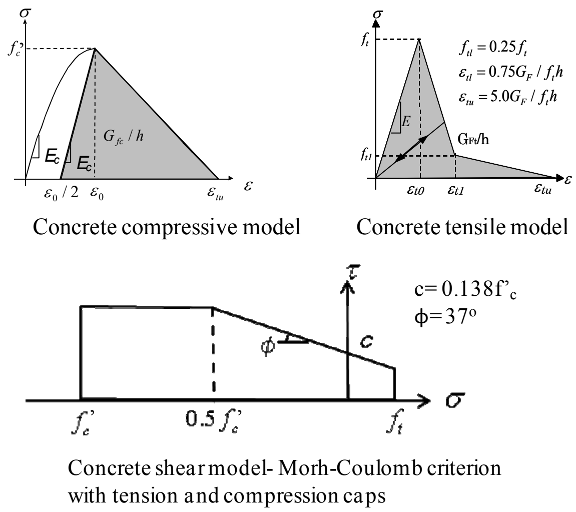

Figure 9. Concrete material model.

3.3 *Corrosion expansion model*

Modeling expansion of corrosion products is shown in Figure 10. Three phase material model including rebar, corrosion products and concrete is applied. The merit of the model is that the properties of corrosion products such as thickness (H) and elastic modulus (E_r) are assumed directly. The model is efficient to investigate the effect of corrosion products. In the model, initial strain is gradually increased in normal springs located on boundary of the corrosion products layer based on initial strain problem.

Ludgren K.(2002), Oh et al. (2009) suggested a model of deformation around rebar due to corrosion products which can be described as shown in Figure 11, in which r, x, U and U_{cor} are initial radius of rebar, corrosion penetration depth, free increase of the radius and the real increase of the radius respectively. The strain in the corrosion products is

$$\varepsilon_{cor} = \frac{U_{cor} - U}{x + U} = \varepsilon_{real} - \varepsilon_{free} \tag{5}$$

In RBSM model, initial thickness of corrosion products layer is modeled constantly as H so

$$\varepsilon_{free} = \frac{U}{H} \tag{6}$$

This parameter is input data in the analytical program through increasing of corrosion rate. U is computed from the corrosion rate as the following equation (Matsuo et al. 1997)

$$U = \frac{W_r(dV - 1)}{\rho_s} \tag{7}$$

where W_r is corrosion rate (mg/cm^2),dV is volume expansion ratio of corrosion products (=2.5, in this study), ρ_s is rebar density (=7.85x10^3 mg/cm^3).

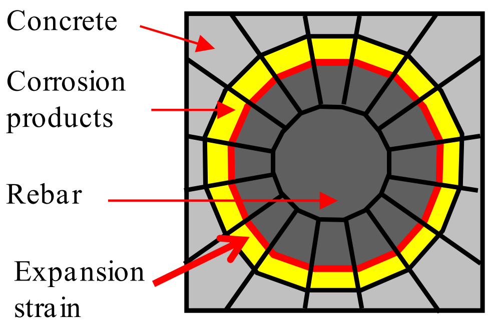

Figure 10. RBSM corrosion expansion model.

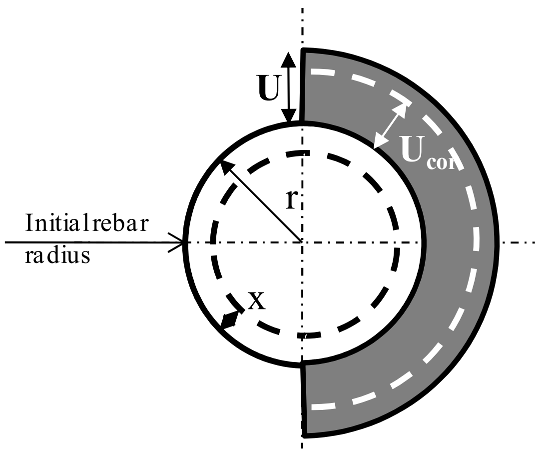

Figure 11. Deformation around rebardue to corrosion products.

It may not be easy to measure properties of corrosion products such as thickness and linear elastic modulus by experiment. We have tried to analyze specimens with various values of the initial thickness and the linear elastic modulus of the corrosion products layer. As the results, the initial thickness (H) 1.0mm and the elastic modulus (E_r) 500MPa can simulate reasonable cracking behaviors in terms of crack patterns and surface crack width propagation in comparison with the experimental results.

4 ANALYTICAL RESULTS

In the analysis, mesh sizes of Voronoi particles are 5mm in the cover area and 10mm in the others. Another arrangement of Voronoi particles is also tried to confirm the similarity of analytical results.

4.1 *Simulation of internal crack patterns*

Analytical crack patterns at several values of the surface crack widths are obtained for type C30 specimens. The analysis is done with two values of the linear elastic modulus of corrosion products 500MPa and 100MPa to compare the effect of this property to internal crack patterns. Figure 12 shows the internal crack patterns when E_r is 500MPa and Figure 13 shows the patterns when E_r is 100MPa.

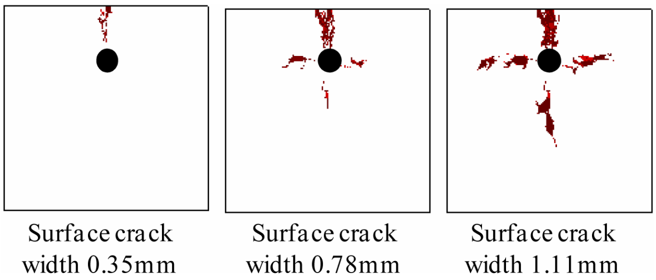

Figure 12. Type C30 crack patterns (**Er=500Mpa**).

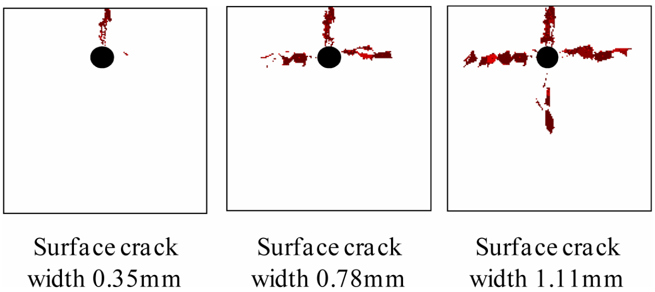

Figure 13. Type C30 crack patterns (**Er=100Mpa**).

With the different values of the elastic modulus E_r, the crack patterns are different but the differences are small. In comparison with the experimental results in Figure 5, the value 500 MPa can simulate better crack patterns of the inside crack when the surface crack width is 0.78mm and 1.11mm. The crack patterns of vertical crack and lateral cracks are similar.

In the case of type C10, we also analyze specimen with the two values 500MPa and 100MPa of the elastic modulus E_r. Analytical crack patterns at surface crack width 0.5mm are shown in Figure 14. As well as in the case of type C30 specimen, the value 500MPa of elastic modulus of corrosion products can simulate the crack pattern more closely to the experimental result (Fig. 6) with two cracks appearing in the concrete cover.

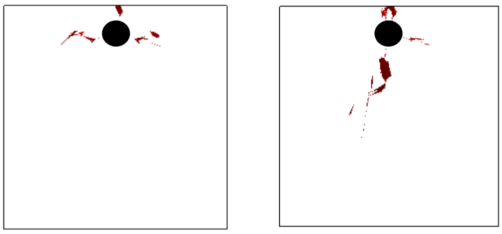

Figure 14. Type C10 crack pattern (surface crack width 0.5mm).

4.2 *Simulation of surface crack width propagation*

Analytical results in the case of type C30 are compared with experimental results as shown in Figure 15. The analytical results appear reasonably agreement with the experimental results, i.e. initiation crack widths occurring with a certain amount of corrosion products and then crack opening propagating speedily up. However, analytical values show larger surface crack widths than the experimental results, especially when corrosion rates increase.

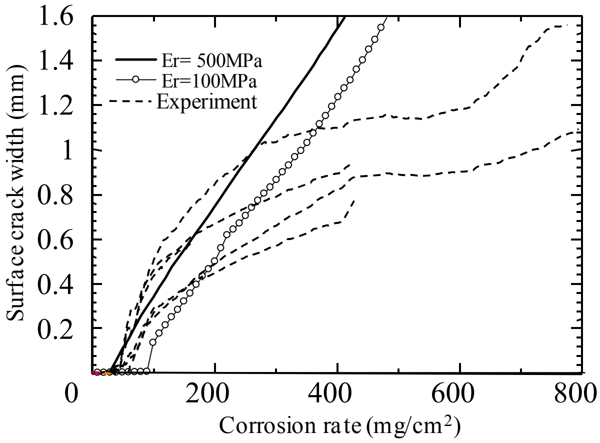

Figure 15. Analytical surface crack width propagation (Type C30).

With a higher value of the linear elastic modulus of the corrosion products, E_r=500MPa, corrosion expansion pressure induced by corrosion products is larger and it causes initiation of surface crack width quicker than the smaller case, E_r =100 MPa. In the early stage of corrosion, the surface crack width in the case of E_r =500 MPa is closer to the experimental results than the one in the case of E_r=100MPa.

4.3 *Penetration of corrosion products into cracks*

During the corrosion process, it is known that corrosion products can penetrate into cracks in concrete so this effect may reduce corrosion expansion pressure on concrete accordingly as shown in Figure 16 (Val et al. 2009, Toongoenthong & Maekawa. 2004).

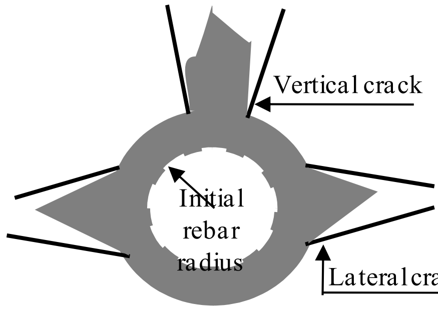

Figure 16. Penetration of corrosion products into cracks.

This effect has been simulated in the RBSM analytical program. One of the advantages of RBSM model is that crack widths and volume of cracks can be calculated directly during the analysis (Fig. 17). It is therefore convenient to calculate reduction of volume of corrosion products which penetrate into cracks. The reduction of corrosion expansion pressure due to the penetration of corrosion products into cracks is calculated by reducing the free increase U in the corrosion expansion model as shown in Figure 18.

We have assumed the following when considering this effect in the analysis:

- Corrosion products can only penetrate into cracks if crack widths exceed the threshold value of crack width.
- Corrosion products fully fill in the cracks
- The free increase U is uniformly reduced around the rebar.

With a free increase of U, the corresponding corrosion product volume V_{cor} is (Figure 18a):

$$V_{cor} = \left[\pi(r+U)^2 - \pi r^2\right]L = \pi U(2r+U)L \qquad (8)$$

since $U^2 \approx 0$, equation (7) can be approximated as

$$V_{cor} = 2\pi r \cdot U \cdot L \qquad (9)$$

where L is the length of rebar.

When the penetration of corrosion products into cracks is considered, the effective corrosion products volume $V_{cor,eff}$ is:

$$V_{cor,eff} = V_{cor} - V_{crk}$$

(10)

where V_{crk} is volume cracks as computed in Figure 17.

If the effective free increase is U_{eff}, the effective volume of corrosion products in Figure 18b will be (similar to (9))

$$V_{cor,eff} = 2\pi . r . U_{eff} . L$$

(11)

from (9),(10) and (11):

$$2\pi.r.U_{eff}.L \;= 2\pi.r.U.L - V_{crk} \tag{12}$$

$$U_{eff} \;= U - \frac{V_{crk}}{2\pi.r.L} \tag{13}$$

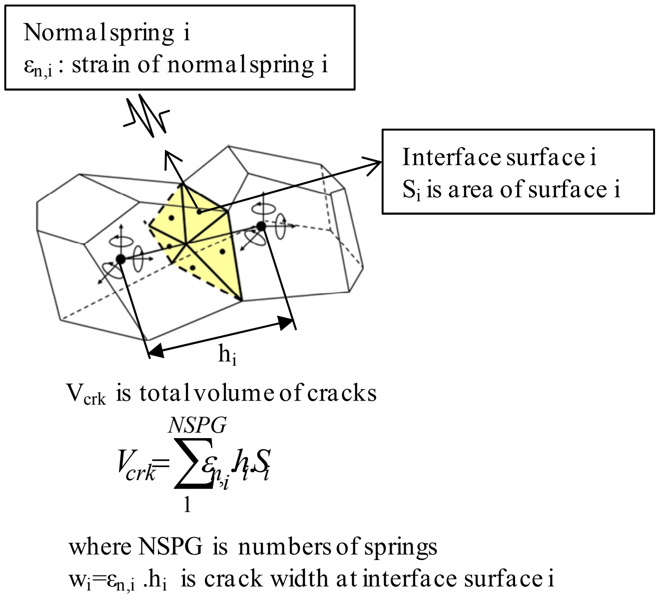

Figure 17. Computation volume of cracks in RBSM model.

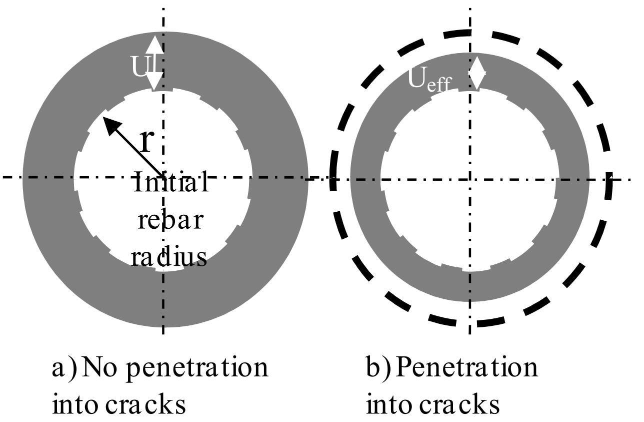

Figure 18. Computation reduction of free increaseU due to penetration of corrosion products into cracks.

Figure 19 shows the propagation of surface crack width when this effect is considered for type C30 specimen. Thresholds of 0.1mm and 0.2mm crack width are considered. The value of 500MPa is used for the elastic modulus of the corrosion products.

It can be seen that the propagation of surface crack width is reasonably agreement with the experimental results when the effect of penetration of corrosion products into cracks is considered.

When the threshold of 0.1mm width is set for the penetration of corrosion products into cracks, the propagation speed of surface of crack width is reduced when the surface crack width grows up to 0.40mm because lateral cracks have occurred and the total volume of cracks becomes large which induces a significant reduction on the corrosion expansion pressure on concrete.

For the case of 0.2mm threshold, the changing point of the propagation is at the value 0.8mm of surface crack width. The tendency of crack width propagation is similar with the case of 0.1mm threshold.

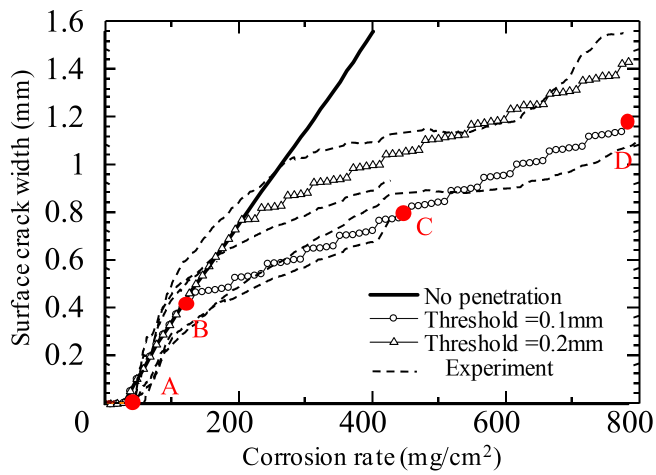

Figure 19. Surface crack width propagation with penetration of corrosion products into cracks.

In comparison with the experimental results, if the threshold of crack width is set between 0.1mm and 0.2mm, it can reasonably simulate the surface crack width propagation as shown in Figure 19.

However, it is noted that in the experiment, corrosion products may not fully penetrate into cracks and the speed of penetration also depends on crack widths and properties of corrosion products. In the analysis, we have assumed the fastest and biggest penetration which induces the largest reduction on corrosion expansion.

The threshold of penetration greatly affects the propagation of surface crack width. The above assumptions are also simple cases for the analysis in this study and it will definitely require further work to simulate the effect to the corrosion process. Especially, it will need further experimental results to verify the simulation results.

4.4 *Simulation of internal crack propagation*

It is necessary to simulate internal crack propagation to predict internal cracking behavior from the surface cracks. Analytical results of propagations of crack width near the rebar, lateral crack length and lateral crack width are compared with the experimental results. The effect of penetration of corrosion products into cracks where crack width is larger than 0.10mm is considered.

4.4.1 *Propagations of crack width of vertical crack near rebar*

The crack width of vertical crack near the rebar as shown in Figure 20 is smaller than the surface crack width at the same level of corrosion rate as shown in Figure 19.

The propagation of crack width near rebar also appears reasonably agreement with the experimental values when the effect of penetration of corrosion into cracks is taken into account

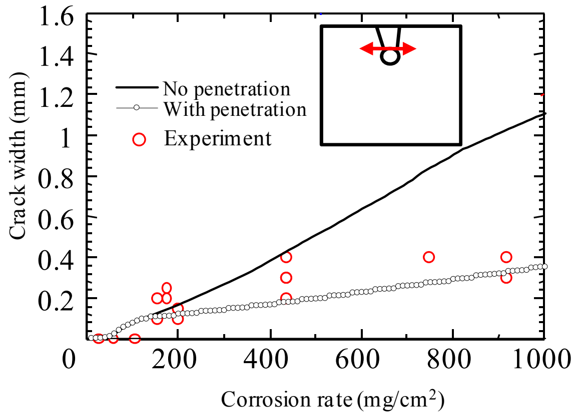

Figure 20. Propagation of vertical crack width nearrebar.

4.4.2 *Propagations of lateral crack length*

The analytical lateral crack length propagation is shown in Figure 21.

The tendency of analytical result is similar to the testing results. The propagation of lateral crack length is closer to the experiment when the penetration effect is considered.

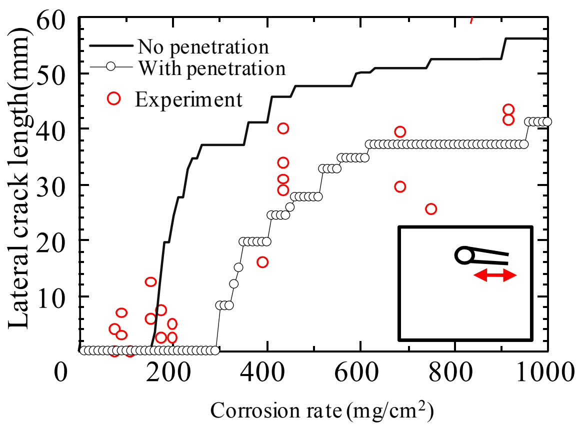

Figure 21. Propagation of lateral crack length.

4.4.3 *Propagations of lateral crack width*

Analytical crack widths of the lateral crack at some positions from the rebar are compared with the experimental results as shown in Figure 22a and 22b. Again, when the effect of corrosion products penetration is considered, the analytical results appear closely to the experimental results.

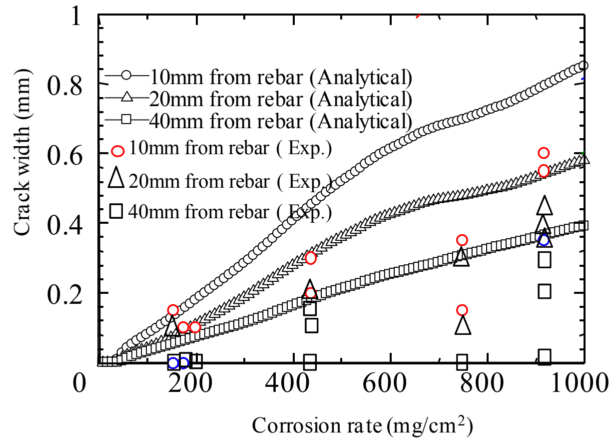

Figure 22a. Propagation of lateral crack width (no penetration).

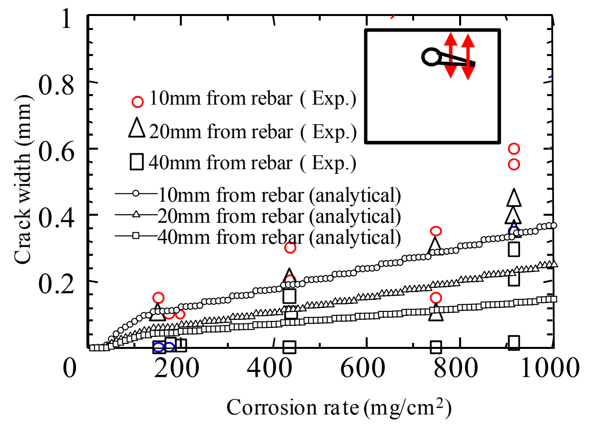

Figure 22b. Propagation of lateral crack width (with penetration).

4.5 *Mechanism of surface crack width propagation with internal crack propagation*

From the surface crack width propagation (Figure 19) and the internal crack propagations (Figure 20, 21,22a and 22b), a mechanism of surface crack width propagation with internal crack propagation can be estimated as shown in Figure 23:

a) Vertical crack initiates from concrete surface (Figure 23a.) and propagates to the rebar corresponding to the stage A to B in Figure 19. In this stage, surface crack width rapidly increases.
b) Then, lateral cracks initiate (Figure 23b.) and increase in their widths and lengths which cause rotation on the concrete parts as shown in Figure 23c. Inside crack initiates (Figure 23c.). Corrosion products penetrate into internal cracks. In this stage, the surface crack width also increases but the speed of surface crack width propagation reduces (stage B to C in Figure 19).
c) With a further amount of corrosion products, the inside crack propagates from the rebar and causes rotation on the concrete parts as shown in Figure 23d. The speed of surface crack width propagation in this

stage (C to D in Figure 19) is slightly higher than the previous stage (B to C).

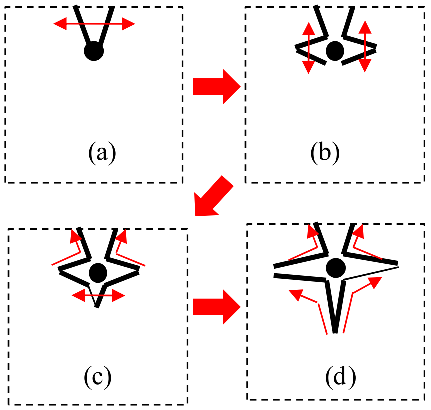

Figure 23. Internal cracking mechanism.

5 CONCLUSIONS

Experiment and 3D- RBSM analytical model was studied to evaluate cracking behavior of the concrete specimen with single rebar.

The three phase material corrosion expansion model was applied in the analysis. The values of initial thickness and linear elastic modulus of corrosion products were recommended.

Internal crack patterns, surface crack width propagation and internal crack propagation were simulated quantitatively and qualitatively and compared with the experimental results. Moreover, the effect of corrosion products penetration into cracks during corrosion process was investigated and it was confirmed that the simulation results were quantitatively agreed with the experimental results when this effect was considered.

Mechanism of surface crack width propagation was clarified and it was strongly dependent on the internal crack propagation. Therefore, in order to evaluate the surface crack propagation, the internal crack propagation must be clarified.

REFERENCES

Andrade, C., Alonso,C.,Molina,F.J.,1993.Cover cracking as a function of bar corrosion: Part I-Experimental test, Materials and Structures, 26: 453-464.

Cabrera,J.G.,1996.Deterioration of Concrete Due to Reinforcement steel Corrosion, Cement & Concrete Composites 18:47-59.

Kawamura,K.,Nakamura,H.,Kunieda,M.,Ueda,N.,2009.A fundamental study about the evaluation of crack propagation in concrete induced by rebar corrosion (in Japanese), Proceeding of JCI meeting, Japan Concrete Institute, CD:1075-1080.

Lundgren,K.,2002, Modeling the effect of corrosion on bond in reinforced concrete, Magazine of Concrete Research,54,No.3:165-173.

Matsuo, T., Nishiuchi, T., Matsumura, T.,1997.Crack Propagation Analysis in Concrete induced by Rebar Corrosion Expansion (in Japanese), Concrete Journal, Japan Concrete Institute,19:99-104.

Nguyen,Q.T.,Millard,A.,Care,S.,L'Hostis,V.,Berthaud,Y.,2006 .Fracture of concrete caused by the reinforcement corrosion products, J.Phys.IV France 136:109-120.

Oh,B.H., Kim,K.H.,Jang, B.S.,2009.Critical corrosion amount to cause cracking of reinforced concrete structures, ACI Material Journal,V,106,No.4:333-339.

Saito, S.,1999.Fracture analyses of structural concrete using spring network with random geometry, Doctoral thesis, Kyushu University.

Toongoenthong,K.,Maekawa,K. 2005.Simulation of coupled corrosive product formation, migration into crack and propagation in reinforced sections, Journal of Advanced Concrete Technology, Vol.3, No.2:253-265.

Tran,K.K., Kawamura,K.,Nakamura,H.,Kunieda,M.,2009. Prediction Of Cracking Of Concrete Due To Rebar Corrosion Using 3D- RBSM, Proceedings of the Eleventh International Summer Symposium, JSCE: 249-252.

Val,V. D., Chernin,L., Stewart,G.M.,2009.Experimental and Numerical Investigation of Corrosion-Induced Cover Cracking in Reinforced Concrete Structures, Journal of Structural Engineering, ASCE, 135:376-385.